

# Spin screening of magnetization due to inverse proximity effect in superconducting/ferromagnetic bilayers

V. Shelukhin<sup>1</sup>, J. Xia<sup>2</sup>, A. Tsukernik<sup>3</sup>, M. Karpovski<sup>1</sup>, A. Kapitulnik<sup>2,4</sup>,  
and A. Palevski<sup>1</sup>

<sup>1</sup>*School of Physics and Astronomy, Tel Aviv University, Tel Aviv 69978, Israel*

<sup>2</sup>*Department of Physics, Stanford University, Stanford, California 94305, USA*

<sup>3</sup>*The Center for Nanoscience and Nanotechnology, Tel Aviv University, Tel Aviv 69978, Israel*

<sup>4</sup>*Department of Applied Physics, Stanford University, Stanford, California 94305, USA*

## 1. Introduction

When ferromagnetic (F) films are deposited on top of superconductors (S) they acquire certain superconducting properties. This is the well-known proximity effect which gives rise to a number of spectacular phenomena<sup>1,2</sup>: superconducting critical current oscillations versus the thickness of the ferromagnet, long range triplet superconductivity, etc. These effects have been already observed experimentally<sup>3-5</sup>. However, the inverse proximity effect<sup>6,7</sup>, namely when the superconductor inherits the ferromagnetic properties is the subject which so far has not attracted as much attention by the experimentalist. Here, we present the transport and optical studies of the inverse proximity effect in superconductor ferromagnetic bilayers. We have measured magnetoresistance of an e-beam lithographically patterned 200 nm thick Pb discs with diameters in the range 2–5  $\mu\text{m}$ , deposited on top of a 5 nm Ni film. Magneto-optical measurements of the polar Kerr effect using a zero-area-loop Sagnac magnetometer on Pb/Ni and Al/(Co-Pd) proximity-effect bilayers show unambiguous evidence for the "inverse proximity effect," in which the ferromagnet (F) induces a finite magnetization in the superconducting (S) layer<sup>8</sup>.

## 2. Theory of inverse proximity effect: reduction of the magnetization due to superconductivity

There are two different mechanisms leading to the reduction of the total magnetization in **SF** structures with itinerant ferromagnets below the superconductor transition temperature  $T_c$ . The first mechanism<sup>6,7</sup> is due to the reduction of the magnetization in the ferromagnet, and the second one is due to the induced magnetization<sup>6,7</sup> in the superconductor in the direction opposite to magnetization in **F**-layer. The reduction of the magnetization in

F-layer is caused by the reduction in the density of states in the ferromagnetic material, and it leads to a very small effect for a strong itinerant ferromagnet with exchange energy being much larger than superconductor gap.

The induced magnetization in the superconductor is a much larger effect<sup>6,7</sup>, which can completely screen the magnetization of a magnetic layer if the thickness of the latter is smaller than its magnetic length. Below  $T_c$ , the Cooper pairs of electrons with opposite spins and typical distance  $\xi_s$  between them form the superconducting state. If the magnetization is homogeneous in the ferromagnet (no rotation) then the condensate function penetrating the ferromagnet due to proximity effect is a mixture of the singlet and triplet components with zero projection of the total spin, and can be viewed as electron pairs with opposite spins just like in the case without F layer. It is clear that when both electrons forming the pair are in the S material they can not contribute to the magnetization. Some pairs, however, are distributed in a more complicated manner, namely one electron is in the ferromagnet whereas another one is in the superconductor. The spin of the electron in the F-layer is aligned along the direction of the magnetization for an itinerant ferromagnet; therefore the spin of another electron will have an opposite direction contributing to a magnetic moment induced in the superconductor. This is of course an oversimplified description, however, it explains the results obtained by a rigorous calculation in the limit when the thickness of the ferromagnet is smaller than the magnetic length.

At zero temperature and for the ideal interface in SF structure the magnetization of the ferromagnet is completely screened<sup>6,7</sup>. This spin screening effect should not be confused with the Meissner effect. The latter is an orbital effect which produces the diamagnetic moment in the superconductor screening the external magnetic field. The induced magnetization in the superconductor due to the spin screening considered in this paper takes place in the S/F structures even if the magnetization in the ferromagnet does not produce magnetic field in the superconductor. As an example, one can consider an infinite plane of magnetic material with the magnetic moment perpendicular to the plane in contact with the plane of the superconductor. The magnetic field in the material of certain geometry  $B_{in}$  in the presence of external magnetic field  $B_{ext}$  and magnetization  $\mathbf{M}$  in the material  $B_{in} = B_{ext} + (1-K)\mu_0\mathbf{M}$  depends on the value of the demagnetization factor  $K$  which is unity  $K=1$  for the infinite plane. Therefore, in the absence of external magnetic field the ferromagnetic thin film magnetized in the direction normal to the plane will not produce magnetic field at any point in real space and thus Meissner diamagnetic moment will not be induced, whereas a diamagnetic moment due to the spin screening will occur as discussed above.

### 3. Samples Fabrication

Samples for both transport and optical measurements were made of thin films of superconductor material deposited on top of thin films of

ferromagnetic material. We used a variety of strong itinerant ferromagnets like Ni, and Pd (3 Å)/Co(9 Å)\*n superlattice structure with  $n \sim 10$ . Strong ferromagnet like Ni has a magnetic length  $L_M \sim 1$  nm and it is appropriate for the studies of the induced magnetization. The ferromagnetic layers were deposited onto SiO<sub>2</sub> and /or GaAs substrate by e-gun evaporation in a vacuum deposition system at the pressure of  $2 \times 10^{-7}$  torr. The thickness of the magnetic films ranged between 2 nm to 10 nm.

The superconductors like Al with a large superconductor coherence length ( $\xi_s \sim 100$  nm) and Pb with a superconductor coherence length ( $\xi_s \sim 60$  nm), were deposited *in situ* on top of the magnetic layers. This procedure guarantees a good quality of the interface between the **S**- and **F**- layers. The thickness of the superconductor films was somewhat larger than  $\xi_s$ .

For the transport studies e-beam lithography was used in order to fabricate an array of small superconductor dots on top of the ferromagnetic layer. The lateral dimensions of the dots as well as the separation between them are of the same order as the thickness of the superconductor layers, namely about 100 nm.

#### 4. Transport Experiments

We have measured magnetoresistance of a discontinuous Pb superconductor deposited on the top of a 5 nm Ni film. The Hall effect of the sample above  $T_c$  is shown in **Fig. 1(a)** and the HRSEM micrograph of the sample is shown in **Fig. 1(b)**.

We see from **Fig. 1(a)** that the Hall effect curve exhibits relatively wide hysteresis. From this measurement of the Hall effect we conclude that Ni is fully magnetized in out-of-plane direction. Otherwise the remnant magnetization at zero external magnetic field would be smaller than the saturated magnetization at large fields, due to formation of Ni domains, with preferred in-plane direction of magnetization.

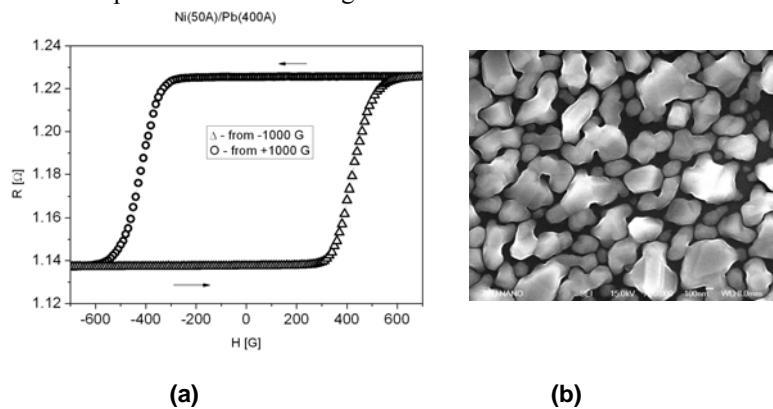


**Figure 1.** (a) Hall effect of Ni/Pb sample above transition temperature (at 9K), two sweeps from -1 kG to +1 kG and from +1 kG to -1kG; (b) HRSEM image of Pb on top of Ni, size of Pb grains: 100 - 500 nm;

From the geometry of the Pb (see *Fig. 1(b)*) one can expect that the demagnetization factor  $K < 1$ , and therefore the magnetic field can be induced if the magnetization appears in Pb below  $T_c$ .

The magnetoresistance curve (see *Fig. 2(a)*) exhibits relatively strong hysteresis ( $\sim 10$  G) in the range of magnetic fields where the magnetization is reversed. This is expected since in this range of fields the Ni film produces a magnetic field, i.e.  $K < 1$  when the domain structure appears. Moreover, a parallel component of the field will also appear and contribute to the increase of the resistance. However, a small hysteresis ( $\sim 4$  G) persists down to zero field, where Ni is fully magnetized (*Fig. 2(b)*). Note that the direction of hysteresis coincides with the direction of magnetization in Ni. It means that the field induced in Pb has opposite direction to Ni magnetization, and could be a result of **the magnetization induced in Pb**.

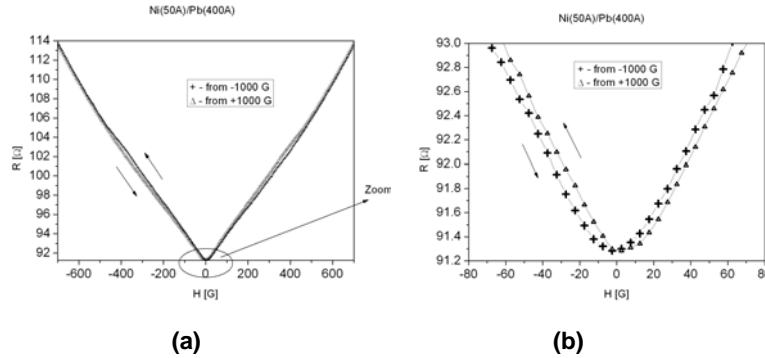


**Figure 2.** (a) magnetoresistance curve of Pb/Ni bilayers at 4.2 K; (b) zoomed part marked with the oval at low fields.

We, of course, can not make any definite statement that the observed hysteretic shifts arise from the inverse proximity effect, however, this experiment indicates that this transport method is sensitive enough to measure local magnetization.

To demonstrate further the relevance of this method we utilized the artificially prepared superconductor dots with much smaller demagnetization factor than that of Pb used in the above experiment. We have measured magnetoresistance of a e-beam lithographically patterned 200 nm thick Pb discs with diameters in the range 2-5 microns, deposited on the top of a 5 nm Ni (or Co/Pd\*12) film. The HRSEM images of the samples are shown below, *Fig. 3*.

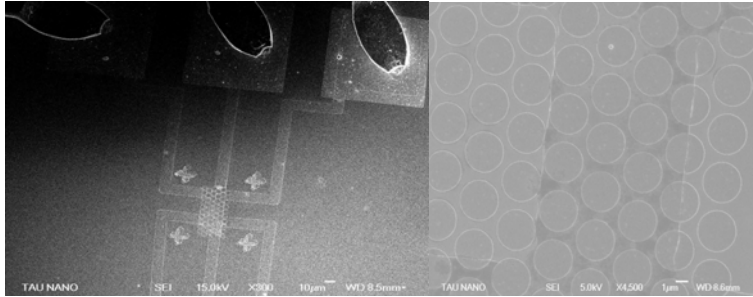


**Figure 3.** HRSEM image of Pb discs on top of Co/Pd\*12 strip.

After measurements of Hall effect above the  $T_c$  of the superconductor (producing results similar to those in *Fig. 1(a)*), the samples were cooled below  $T_c$  for the induced magnetization experiments. In order to remain sensitive to the induced magnetization we could not cool below  $0.9 T_c$ , because at lower temperatures the critical magnetic field of the Pb discs was too high to perform relevant magnetoresistance measurements.

The magnetoresistance curve of 5  $\mu\text{m}$  and 3  $\mu\text{m}$  diameter Pb discs on top of Ni film are shown in *Fig. 4. (a)* and *(b)*. Both curves exhibit relatively strong anomalous hysteresis of about 3 G and 7 G respectively. The direction of the hysteresis coincides with the direction of magnetization in Ni, indicating that the field induced in Pb has opposite direction to Ni magnetization, and it is a result of the magnetization induced in Pb.

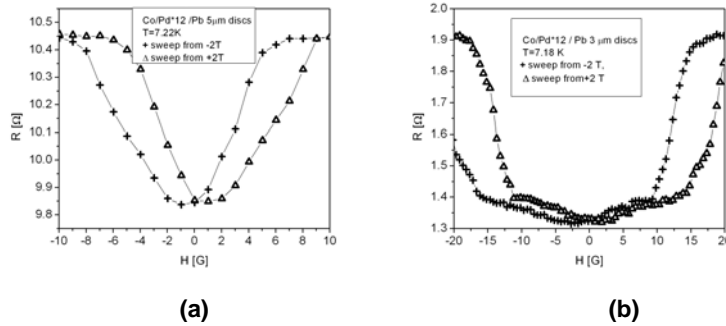


**Figure 4.** (a) magnetoresistance of the Pb (5 $\mu\text{m}$  diameter, 200nm thick discs) on Co-Pd\*12 multilayer at superconducting transition temperature, 7.22 K; (b) magnetoresistance of the Pb (3 $\mu\text{m}$  diameter, 200 nm thick discs) on Co-Pd\*12 multilayer near the superconducting transition temperature,  $T=7.18$  K

The effect we observe in the fabricated array of superconducting discs essentially is the same as observed in semi continuous Pb films, *Fig. 2* The hysteresis increases as the diameter of the superconductor Pb disc decreases. This is expected since the demagnetization factor is reduced when the ratio of the height of the disc to its diameter is decreased. It is difficult to measure

temperature dependence of the hysteresis because after transition to superconducting state below  $T_c$  the critical magnetic

### Optical measurements

Ni-Pb and Co-Pd/Al bilayers, with superconductor temperatures  $T_c \approx 6.5$  K for Pb/Ni and  $T_c \approx 0.6$  K for Al/Pd-Co structures were mounted into the novel apparatus that was built at Stanford University<sup>9</sup> for Polar Kerr Effect (PKE) measurements, **Fig.5**.

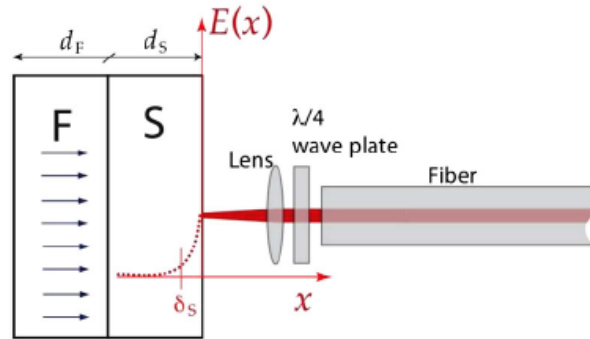


**Figure 5.** Cartoon of the measuring set-up for PKE

Our samples of typically 5 mm X 5 mm size were mounted on a copper plate of the cryostat using GE varnish for magneto-optical studies at low temperatures. The system was aligned at room temperature, focusing the beam that emerges out of the quarter-waveplate to a  $3 \mu\text{m}$  size spot in the middle of the samples. Polar Kerr effect measurements were performed using a zero-area-loop polarization-Sagnac interferometer at wavelength of 1550 nm. The light is reflected from the superconductor film of our samples which is a top layer in our structures. Typical performance was a shot-noise limited  $0.1 \mu\text{rad/pHz}$  at  $10 \mu\text{W}$  of incident optical power from room temperature down to 0.5 K. The samples were first cooled at zero external fields to about 10 K. At this temperature an external magnetic field of 6 Tesla normal to the films' plain was applied to magnetize the ferromagnetic layer in the direction of the applied magnetic field and after that the field was turned off at the same temperature, well above the superconductor transition. The samples were cooled to the lowest temperature 0.5 K at zero magnetic fields and the Kerr effect of the samples were measured while the samples were warmed from 0.5 K to the temperatures exceeding superconductor  $T_c$ . **Fig. 6** shows the Kerr effect measured on both Pb/Ni (**a**) and Al/Co-Pd (**b**) samples. Both graphs clearly show the onset of Kerr angle variation versus the temperature at a certain value of the temperature which according to our transport studies coincides with the superconductor transition temperature  $T_c$ .

The sign of the Kerr angle detected in our measurement corresponds to the direction of the magnetization in superconductor opposite to the direction of magnetization in the ferromagnetic layer. This diamagnetic response is expected for the inverse proximity effect in the diffusive limit<sup>6</sup>.

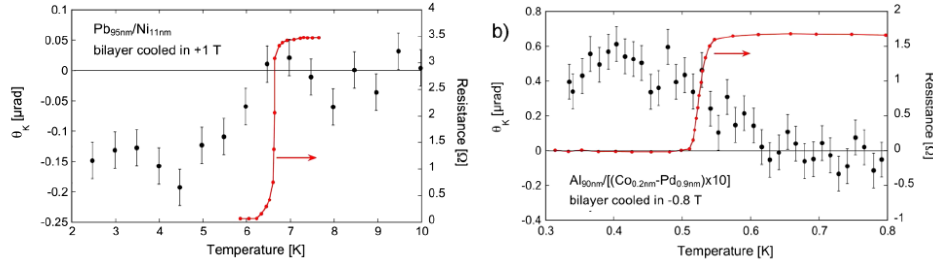


**Figure 6.** Kerr angle versus temperature (dots) and superconducting transition (line) for: (a) Ni/Pb sample; (b) Co-Pd/Al sample.

Pb has much stronger spin-orbit coupling than Al. Nevertheless, the Kerr angle rotation we observe in Al is almost by order of magnitude larger than in Pb. Our estimate of the Kerr angle due to Meissner diamagnetism gives value even for Pb below the detection limit of our apparatus. Therefore, the diamagnetic response observed in our samples must have a spin origin, and it is induced in the superconductor layer by spin screening due to inverse proximity effect.

## 5. Conclusions

Inverse proximity effect in SF structures (Pb/Ni and Al/Co-Pd) by transport and optical methods were investigated. The results obtained in both transport and optical studies of the inverse proximity effect strongly indicate that the signals (rotation of the polarization angle of light and the hysteresis) arise from spin induced magnetization. The increase of the Kerr angle as the temperature is lowered through the superconductor transition temperature follows the theoretically predicted curve and therefore should be considered as direct experimental evidence for the phenomenon called "spin screening" due to proximity effect in S/F bilayers.

## Acknowledgments

This work was supported by the US-Israel Binational Science Foundation (BSF) Grant 2006010 and Israel Science Foundation Grant 530/08; NSF NSEC Grant 0425897; Department of Energy Grant DE-AC02-76SF00515.

## References

1. A. I. Buzdin, Rev. Mod. Phys. **77**, 935 (2005).
2. F.S. Bergeret, A.F. Volkov, K.B. Efetov, Rev. Mod. Phys. **77**, 1321 (2005).
3. V.V. Ryazanov, V. A. Oboznov, A. Yu. Rusanov, A.V. Veretennikov, A. A. Golubov, and J. Aarts, Phys. Rev. Lett. **86**, 2427 (2001).
4. Y. Blum, A. Tsukernik, M. Karpovski, and A. Palevski, Phys.Rev. Lett. **89**, 187004 (2002).
5. R. S. Keizer et al., Nature (London) 439, 825 (2006).
6. F. S. Bergeret, A. F. Volkov, and K. B. Efetov, Europhys. Lett. 66, 111 (2004).
7. M.Y. Kharitonov, A. F. Volkov, and K. B. Efetov, Phys. Rev. B 73, 054511 (2006).
8. Jing Xia, V. Shelukhin, M. Karpovski, A. Kapitulnik, and A. Palevski, Phys. Rev. Lett. 102, 087004 (2009)
9. Jing Xia, P. T. Beyersdorf, M. M. Fejer, and A. Kapitulnik, Appl. Phys. Lett. 89, 062508 (2006).